Mon. Not. R. astr. Soc. (1987) **227**, 975–992

Stabilization of non-axisymmetric instabilities in a rotating flow by accretion on to a central black hole

O. M. Blaes *Theoretical Astrophysics 130–33, California Institute of Technology, Pasadena, CA 91125, USA*

Accepted 1987 March 24. Received 1987 February 25

Summary. The normal modes of a sequence of two-dimensional flows around a black hole are investigated. When the flow is one of pure rotation, numerous non-axisymmetric dynamical instabilities are found which are similar to those discovered by previous authors. When the inner edge of the flow crosses the critical 'cusp' radius, a purely rotating equilibrium flow is no longer possible and the fluid in the inner regions flows into the hole transonically. All the unstable modes found for the purely rotating flow are quickly stabilized by this process. The relevance of these results to the dynamical stability of accreting thick tori is discussed.

1 Introduction

Geometrically thick, pressure supported accretion discs rotating around supermassive black holes have recently been among the more fashionable theoretical models of quasar and active galactic nuclei central engines (see e.g. Rees 1984, and references therein). However their viability has been put under serious question with the discovery (Papaloizou & Pringle 1984) that they may be dynamically unstable. Specifically, it was shown that perfect fluid, isentropic, non-self-gravitating tori rotating with constant specific angular momentum are unstable in the linear regime to global non-axisymmetric perturbations. It was then claimed that these instabilities were likely to persist in more general classes of tori. Since then, much work has been done and continues to be done in checking this statement by investigating arbitary rotation laws and entropy distributions and in trying to understand the physical causes and consequences of these instabilities.

Because of their simpler geometry, very slender barotropic tori have been the subject of much analytic and quasianalytic attack (Papaloizou & Pringle 1985; Blaes 1985; Blaes & Glatzel 1986; Goldreich, Goodman & Narayan 1986). They are unstable to essentially two-dimensional modes which can be understood in terms of an interaction between surface waves rotating around the inner and outer edges of the torus. In the non-linear regime these modes cause the torus to break up into planet-like blobs (Hawley 1987; Goodman, Narayan & Goldreich 1986). However they are stabilized if the torus is thick enough or the specific angular momentum gradient is steep enough (Goldreich, Goodman & Narayan 1986).

Calculations of the normal modes of two-dimensional differentially rotating annuli by Glatzel (1987) and the fastest growing modes in thick tori by Kojima (1986a, b) and J. Frank (private communication) show that other unstable modes exist in thicker configurations. Surprisingly, the two- and three-dimensional calculations show remarkable qualitative similarities, the principal difference being that in the case of tori the growth rates become small as the torus becomes very thick, while in the case of annuli the growth rates do not show any comparable decrease. Again, some of the modes are stabilized by steep enough angular momentum gradients, but other, more slowly growing modes still survive. J. Frank (private communication) has also considered truly baroclinic tori, but has not been able to find an absolutely stable configuration.

Finally, WKB analyses of two-dimensional systems and thin discs by Goldreich & Narayan (1985); Drury (1985); Loska (1986); Papaloizou & Pringle (1987); Narayan, Goldreich & Goodman (1987) and Kato (1987) have emphasized the importance of outward angular momentum transport across a corotation point as the driving force behind these instabilities and examined the physical conditions whereby this occurs.

The general picture which emerges from these results is that differentially rotating tori may always be linearly unstable, and so an investigation of the non-linear growth is essential to determine whether or not thick discs can exist. Zurek & Benz (1986) have published the only fully three-dimensional non-linear hydrodynamical calculations so far, the main results being that tori which initially rotate with constant specific angular momentum undergo violent dynamical evolution to configurations which rotate with an average specific angular momentum gradient which is steeper. These in turn undergo dynamical evolution on a longer time-scale.

Much more useful work remains to be done along these lines, particularly the non-linear calculations. All of these results concern only tori which have no other motion apart from rotation, however. Stationary thick *accretion* discs are envisaged to have a cusp at their inner edges through which material falls transonically into the black hole (Paczynski & Wiita 1980; Abramowicz & Zurek 1982). No viscosity is necessary for this process as it is purely a consequence of general relativity. Abramowicz, Blaes & Lu (1986) speculated that this could have an important effect on the instability, especially as the linear calculations for the fastest growing modes in thick Newtonian tori all have eigenfunctions concentrated towards the inner edge. These modes form resonant cavities of negative angular momentum in the inner region, and it is the leakage of positive angular momentum through corotation into the outer parts of the torus which drives the unstable growth (Goldreich & Narayan 1985; Narayan, Goldreich & Goodman 1987). For such modes the transonic accretion flow could clearly be of great importance in damping the instability by advecting negative angular momentum out of the inner regions through the cusp.

Unfortunately, the global linear stability of an accreting thick disc is a very difficult problem. To get around this, we simplify matters by completely ignoring the vertical dimension and considering two-dimensional flows. While making the problem much more tractable, it also of course artificially enhances the stabilizing effects of accretion, a fact which should be kept in mind and will be discussed further below.

Given this drastic assumption, it hardly seems necessary to treat the spacetime of the black hole accurately. Instead, we simplify much of the algebra by adopting the pseudo-Newtonian potential of Paczynski & Wiita (1980). A full general relativistic treatment would only produce changes in the magnitudes of the normal mode eigenfrequencies due primarily to the gravitational redshift. Otherwise no qualitative differences arising from this assumption are expected.

In Section 2 the stationary flow structure will be derived and discussed. Then the perturbation equations will be derived in Section 3 followed in Section 4 by an analytic calculation of the normal modes of a slender ribbon. This gives a starting point for the numerical calculations of Section 5 where unstable modes are calculated for both accreting and non-accreting flows. The cause of these instabilities is best understood in terms of angular momentum transport which will be examined in Section 6 followed finally by a discussion of the results and some conclusions.

2 Stationary flow structure

Consider first a two-dimensional, stationary axisymmetric flow with non-zero radial velocity v_r. Assuming the fluid is ideal, the flow must have constant specific entropy and specific angular momentum l. It is therefore a potential flow and its structure is given by solving the Bernoulli and continuity equations:

$$\frac{1}{2}v_r^2+\frac{l^2}{2r^2}+\frac{(n+1)p}{\varrho}+\Phi=E \tag{2.1}$$

and

$$r\varrho v_r=-\dot{M} \tag{2.2}$$

where r is the distance from the centre, p the pressure, ϱ the density, Φ the gravitational potential and E and $\dot{M}$ are constants, the latter being proportional to the radial mass flux. The fluid is assumed to obey a polytropic equation of state

$$p=K\varrho^{\gamma}=K\varrho^{1+1/n} \tag{2.3}$$

and, as mentioned previously, a pseudo-Newtonian potential is adopted:

$$\Phi=\frac{-GM}{r-R_G} \tag{2.4}$$

where $R_G=2GM/c^2$ is the Schwarzschild radius. The self-gravity of the fluid is assumed to be negligible. It is covenient to express ϱ and p in terms of the sound speed

$$a=\left(\frac{\gamma p}{\varrho}\right)^{1/2} \tag{2.5}$$

and to scale length with R_G and time with R_G/c. Then equations (2.1) and (2.2) may be rewritten in the form

$$\frac{1}{2}v_r^2+na^2=E+\frac{1}{2(r-1)}-\frac{l^2}{2R^2} \tag{2.6}$$

and

$$ra^{2n}v_r=-\dot{\mathscr{M}} \tag{2.7}$$

where $\dot{\mathscr{M}}=\dot{M}(\gamma K)^n=$ constant. Equations (2.6) and (2.7) are identical, apart from the geometry, to those considered by Abramowicz & Zurek (1982) in their study of 'conical' accreting flows. At very large radii, the infall velocity will tend to zero and the flow will be subsonic. Close to the horizon, however, v_r will be very large and the flow will be supersonic. The transition radius r_s between these two regimes (the 'sonic point') is a critical point of equations (2.6) and (2.7). Following Abramowicz & Zurek (1982), one can show that the requirement that the flow be non-singular there determines the two constants $\dot{M}$ and E:

$$\dot{\mathscr{M}}=r_s\left\{\frac{1}{r_s^2}[l_{\text{kep}}^2(r_s)-l^2]\right\}^{n+1/2} \tag{2.8}$$

$$E=\frac{(n+1/2)r_s}{2(r_s-1)^2}-n\frac{l^2}{r_s^2}-\frac{1}{2(r_s-1)} \tag{2.9}$$

where

$$l^2_{\rm kep}(r)=\frac{r^3}{2(r-1)^2} \tag{2.10}$$

is the 'Keplerian' distribution of specific angular momentum, i.e. the distribution corresponding to free particle circular orbits. Equations (2.6) and (2.7) may then be solved numerically to find the distribution of v_r and a^2 throughout the flow.

Consider now a constant specific angular momentum, isentropic flow which is not accreting, but instead is in a state of pure rotation. This flow is still potential, and so is simply governed by equation (2.6) with $v_r=0$:

$$na^2=E+\frac{1}{2(r-1)}-\frac{l^2}{2r^2}; \tag{2.11}$$

the continuity equation now being redundant. Depending on the values of l and E, equation (2.11) gives the equilibrium structure of rotating annuli with varying positions of inner and outer surface radii, given by solving equation (2.11) with $a^2=0$. In these configurations, E is simply minus the binding energy at the surface radii. Such flows are known to be dynamically unstable (Papaloizou & Pringle 1984; Glatzel 1987).

We now construct a one-parameter sequence of these unstable annuli which smoothly joins on to a sequence of unbounded accreting flows. There are a variety of ways to do this, and we choose to fix $l=2$, the Keplerian value at the marginally bound orbit. Each annulus will then have a pressure maximum at radius $r_{\rm kep}=5.236$, given by noting that this is also a Keplerian point in the flow:

$$l^2=\frac{r^3_{\rm kep}}{2(r_{\rm kep}-1)^2}. \tag{2.12}$$

The value of E uniquely determines the flow structure. Zero corresponds to the accretion transition where the flow just reaches from an inner 'cusp' on the marginally bound orbit out to infinity. For $E<0$ the flow is annular and equation (2.11) must be used to determine its structure. Making E more and more negative shrinks the annulus until at

$$E_{\rm min}=\frac{(2-r_{\rm kep})}{4(r_{\rm kep}-1)^2} \tag{2.13}$$

it forms an infinitely slender ribbon rotating at $r_{\rm kep}$. For $l=2$, $E_{\rm min}$ has a numerical value of -0.0451.

For $E>0$, the accretion equations (2.6)–(2.9) are used. Increasing E above zero starts the accretion, with the sonic point moving in from the marginally bound orbit. This entire sequence now permits a study of the effects of accretion on the instabilities.

3 The perturbation equations

Moncrief (1980) has derived the formalism for treating the linear stability of accreting potential flows in both general relativity and Newtonian theory. A useful result from this work is that the perturbed flows will also be potential after a finite time even if perturbations in specific entropy and vorticity are introduced initially over a bounded region of the flow. This is true because in the linear regime the stationary flow acts to advect first the specific entropy and then the vorticity into the hole leaving a purely potential flow behind. Provided these perturbations are not unstable and grow into the non-linear regime before this advection process is completed, then one may assume for the purposes of stability analysis that the perturbed flow is potential from the start.

The linear perturbation equations for non-accreting potential flows were first derived by Papaloizou & Pringle (1984). Here too the perturbed flow is potential provided we neglect initial data corresponding to the continuous spectrum of normal modes associated with a corotation point (Narayan, Goldreich & Goodman 1987; see e.g. Balbinski 1982 for a discussion of these modes in rotating flows).

We therefore assume that the perturbed flows always remain potential and so the perturbation equations may be derived from the time-dependent, non-axisymmetric Bernoulli and continuity equations:

$$\frac{\partial\psi}{\partial t}+\frac{1}{2}v_{\mathrm{r}}^2+\frac{1}{2}v_\phi^2+na^2+\Phi=0 \tag{3.1}$$

$$\frac{\partial\varrho}{\partial t}+\frac{1}{r}\frac{\partial}{\partial r}(r\varrho v_{\mathrm{r}})+\frac{1}{r}\frac{\partial}{\partial\phi}(\varrho v_\phi)=0. \tag{3.2}$$

Here ψ is the velocity potential so the radial and azimuthal components of velocity are given by

$$v_{\mathrm{r}}=\frac{\partial\psi}{\partial r} \tag{3.3}$$

$$v_\phi=\frac{1}{r}\frac{\partial\psi}{\partial\phi}. \tag{3.4}$$

Linearizing equations (3.1) and (3.2) about the stationary flow,

$$\frac{\partial\delta\psi}{\partial t}+v_{\mathrm{r}}\frac{\partial\delta\psi}{\partial r}+\Omega\frac{\partial\delta\psi}{\partial\phi}+n\delta(a^2)=0 \tag{3.5}$$

$$\frac{\partial\delta\varrho}{\partial t}+v_{\mathrm{r}}\frac{\partial\delta\varrho}{\partial r}+\Omega\frac{\partial\delta\varrho}{\partial\phi}+\frac{\delta\varrho}{r}\frac{d}{dr}(rv_{\mathrm{r}})+\frac{1}{r}\frac{\partial}{\partial r}\left(r\varrho\frac{\partial\delta\psi}{\partial r}\right)+\frac{\varrho}{r^2}\frac{\partial^2\delta\psi}{\partial\phi^2}=0 \tag{3.6}$$

where $\Omega=l/r^2$ is the angular velocity of the stationary flow and δ denotes an Eulerian perturbation. The perturbations in density and sound speed squared are related by

$$\frac{\delta\varrho}{\varrho}=n\frac{\delta a^2}{a^2}. \tag{3.7}$$

Hence equation (3.5) may be rewritten

$$\frac{\partial\delta\psi}{\partial t}+v_{\mathrm{r}}\frac{\partial\delta\psi}{\partial r}+\Omega\frac{\partial\delta\psi}{\partial\phi}+a^2\frac{\delta\varrho}{\varrho}=0. \tag{3.8}$$

Finally, on eliminating $\delta\varrho$ between equations (3.6) and (3.8) we obtain a single linear equation for $\delta\psi$:

$$\left(\frac{\partial}{\partial t}+v_{\mathrm{r}}\frac{\partial}{\partial r}+\Omega\frac{\partial}{\partial\phi}\right)\left[\frac{\varrho}{a^2}\left(\frac{\partial}{\partial t}+v_{\mathrm{r}}\frac{\partial}{\partial r}+\Omega\frac{\partial}{\partial\phi}\right)\delta\psi\right]$$

$$+\frac{\varrho}{a^2r}\frac{d}{dr}(rv_{\mathrm{r}})\left(\frac{\partial}{\partial t}+v_{\mathrm{r}}\frac{\partial}{\partial r}+\Omega\frac{\partial}{\partial\phi}\right)\delta\psi-\frac{1}{r}\frac{\partial}{\partial r}\left(r\varrho\frac{\partial\delta\psi}{\partial r}\right)-\frac{\varrho}{r^2}\frac{\partial^2\delta\psi}{\partial\phi^2}=0. \tag{3.9}$$

We now consider normal mode solutions which have time and azimuthal dependence of the form $\exp[i(\sigma t+m\phi)]$, where σ is an unknown complex eigenfrequency and m is a non-zero integer. (Axisymmetric perturbations are considered in the Appendix where they are shown to be stable.) This assumption involves no loss of generality provided the normal modes form a complete set for the representation of the time evolution of any arbitary initial data. For purely rotating flows, the normal modes are, in a useful sense, complete (Dyson & Schutz 1979). The situation for accreting flows, on the other hand, is not well understood. Nevertheless we find that the unstable modes of the purely rotating flow are continuous when the flow starts to accrete so that the normal mode assumption is certainly adequate for our purposes.

Equation (3.9) may now be rewritten as a second order ordinary differential equation for $\delta\psi$:

$$\varrho(a^2-v_r^2)\frac{d^2\delta\psi}{dr^2}+\left(\frac{a^2\varrho}{r}+a^2\frac{d\varrho}{dr}-2i\bar{\sigma}\varrho v_r+\varrho\frac{v_r^2}{a^2}\frac{da^2}{dr}-\varrho v_r\frac{dv_r}{dr}\right)\frac{d\delta\psi}{dr}$$
$$+\left(\bar{\sigma}^2\varrho-\frac{a^2m^2\varrho}{r^2}+i\bar{\sigma}\varrho\frac{v_r}{a^2}\frac{da^2}{dr}-\varrho v_r im\frac{d\Omega}{dr}\right)\delta\psi=0 \tag{3.10}$$

where

$$\bar{\sigma}\equiv\sigma+m\Omega. \tag{3.11}$$

For non-accreting flows ($v_r=0$), this reduces to

$$\varrho\frac{d^2\delta\psi}{dr^2}+\left(\frac{\varrho}{r}+\frac{d\varrho}{dr}\right)\frac{d\delta\psi}{dr}+\left(\frac{\bar{\sigma}^2\varrho}{a^2}-\frac{m^2\varrho}{r^2}\right)\delta\psi=0 \tag{3.12}$$

which is identical to the two-dimensional version of equation (4.1) of Papaloizou & Pringle (1984).

The boundary conditions appropriate to the non-accreting, annular flows are that the Lagrangian perturbation in pressure vanish at the inner and outer radii of the annulus (Tassoul 1978), which in turn implies simply that $\delta\psi$ be regular there. For the accreting flows, the sonic point is a regular singular point of equation (3.10). We therefore again adopt the boundary condition that $\delta\psi$ be regular there.

Boundary conditions must also be applied at infinity for the accreting flows. Expanding equations (2.6) and (2.7) for large r, we find

$$a^2\sim\frac{E}{n}+\frac{1}{2nr}+O\left(\frac{1}{r^2}\right) \tag{3.13}$$

and

$$v_r\sim-\frac{\dot{\mathscr{M}}}{r}\left(\frac{n}{E}\right)^n+O\left(\frac{1}{r^2}\right). \tag{3.14}$$

The asymptotic solution of the peturbation equation (3.10) is then

$$\delta\psi\sim Ar^{-s}\exp\left[\pm i\sigma r\left(\frac{n}{E}\right)^{1/2}\right]\left[1+O\left(\frac{1}{r}\right)\right] \tag{3.15}$$

where A is an arbitrary complex constant and

$$s=\frac{1}{2}+\frac{i\sigma n}{E}\left[\pm\frac{1}{4}(En)^{-1/2}+\dot{\mathscr{M}}\left(\frac{n}{E}\right)^n\right]. \tag{3.16}$$

The plus and minus signs in equations (3.15) and (3.16) correspond to incoming and outgoing waves respectively. In what follows we shall take the minus sign and thus consider only outgoing waves. The same boundary condition has been used by Broadbent & Moore (1979), Glatzel (1987) and Papaloizou & Pringle (1987) in their treatments of unbounded purely rotating flows.

A well-known and useful fact concerning the non-accreting, purely rotating flows is that if $(\delta\psi, \sigma, m)$ is a solution to equation (3.12), then $(\delta\psi^*, \sigma^*, m)$ $(\delta\psi, -\sigma, -m)$ and $(\delta\psi^*, -\sigma^*, -m)$, where the asterisk denotes complex conjugate, are also solutions. These symmetries are useful in reducing the number of solutions which have to be found numerically, but they break down when the flow stars to accrete. Moreover, of these four related complex solutions, only the two which are unstable survive the transition to accretion. These two results arise because the outgoing wave boundary condition and the incoming stationary accretion flow break the time reversal symmetry of the perturbation equations. Indeed, if the sign of v_r was reversed so that we had a subsonic outflow, and if we considered incoming waves at infinity, then only the two damped modes would survive. (The author wishes to thank Peter Goldreich for a helpful discussion of this point).

4 Normal modes of slender annuli

For the purposes of starting an iterative search for numerical solutions to the perturbation equations, it is useful to have a complete analytic solution of all the modes in a limiting case. This is possible to achieve for the infinitely slender annulus, and the method of solution is similar to that of the infinitely slender torus treated by Blaes (1985).

As $E \to E_{\min}$ the inner and outer edges both approach r_{kep}, the central pressure maximum of the annulus where the fluid rotates with the Keplerian angular velocity. Define a small parameter ε such that

$$E = E_{\min} + \varepsilon^2 = \frac{(2 - r_{\text{kep}})}{4(r_{\text{kep}} - 1)^2} + \varepsilon^2. \tag{4.1}$$

Then equations (2.11) and (2.12) imply

$$na^2 = \frac{(2 - r_{\text{kep}})}{4(r_{\text{kep}} - 1)^2} + \varepsilon^2 + \frac{1}{2(r-1)} - \frac{r_{\text{kep}}^3}{4r^2(r_{\text{kep}} - 1)^2}. \tag{4.2}$$

It is now useful to consider a coordinate which shrinks with the annulus as it becomes slender. Such a quantity may be defined by

$$\eta = \frac{r - r_{\text{kep}}}{\varepsilon}\left[\frac{r_{\text{kep}} - 3}{4r_{\text{kep}}(r_{\text{kep}} - 1)^3}\right]^{1/2}. \tag{4.3}$$

Substituting into equation (4.2) and expanding for small ε,

$$na^2 = \varepsilon^2(1 - \eta^2) + \mathrm{O}(\varepsilon^2). \tag{4.4}$$

Hence the surface radii of the annulus occur at $\eta = \pm 1$.

The perturbation equation (3.13) can be re-expressed in terms of a^2 as

$$a^2\frac{d^2\delta\psi}{dr^2} + \left(\frac{a^2}{r} + n\frac{da^2}{dr}\right)\frac{d\delta\psi}{dr} + \left(\bar{\sigma}^2 - \frac{m^2a^2}{r^2}\right)\delta\psi = 0. \tag{4.5}$$

Eliminating r and a^2 using equations (4.3) and (4.4) this becomes, to lowest order in ε,

$$(1 - \eta^2)\frac{d^2\delta\psi}{d\eta^2} - 2n\eta\frac{d\delta\psi}{d\eta} + n(\sigma + m\Omega_0)^2\frac{4r_{\text{kep}}(r_{\text{kep}} - 1)^3}{(r_{\text{kep}} - 3)}\delta\psi = 0 \tag{4.6}$$

where Ω_0 is the angular velocity at r_{kep}. The only solutions of this equation which are regular at the boundaries are Gegenbauer polynomials,

$$\delta\psi = C_N^{n-1/2}(\eta) \tag{4.7}$$

and the corresponding eigenvalues are

$$(\sigma + m\Omega_0)^2 = \frac{N(N+2n-1)}{4nr_{\text{kep}}}\frac{(r_{\text{kep}}-3)}{(r_{\text{kep}}-1)^3} \tag{4.8}$$

or, in terms of pattern speeds,

$$\Omega_{\text{p}} = \Omega_0\left\{1 \pm \frac{1}{|m|}\left[\frac{N(N+2n-1)}{2n}\frac{(r_{\text{kep}}-3)}{(r_{\text{kep}}-1)}\right]^{1/2}\right\}. \tag{4.9}$$

Here N, a non-negative integer, gives the number of nodes of $\delta\psi$ inside the annulus. The plus (minus) sign in equation (4.9) corresponds to modes which rotate faster (slower) than the equilibrium flow. All these modes have real eigenfrequencies and are therefore stable. The $N=0$ mode, however, corotates with the equilibrium flow and is in fact only marginally stable. When the annulus is thickened away from this limit the resulting shear in the flow causes this mode to split into an unstable and damped complex conjugate pair.

The $N=0$ slender annulus modes are in fact equivalent to the unstable modes of a slender torus, the two eigenfrequencies being related by a simple transformation between the two- and three-dimensional polytropic indices (Goldreich, Goodman & Narayan 1986):

$$n_{3\text{D}} = n_{2\text{D}} - ½. \tag{4.10}$$

The only other modes which are equivalent to slender torus modes are the $N=1$ modes, which have identical frequencies to the $j=0$, $k=1$ f-mode which is symmetric with respect to the equatorial plane and has a vertical nodal surface passing through the pressure maximum (see Blaes 1985 for notation). Not surprisingly, these modes along with the corotating mode are the only one for which the perturbed velocity potential is independent of height in the slender torus. One might hope therefore that any instabilities which arise from the $N=0$ or 1 modes in the annulus are also present with very similar pattern speeds and growth rates in three-dimensional tori with the same radial thickness. All other unstable modes will probably not have such counterparts in tori, but nevertheless one expects torus modes which will at least be qualitatively similar.

5 Numerical integrations

Using the slender annulus eigenfrequencies as starting values, we increase E and solve numerically for the new eigenfrequencies by the standard shooting and matching technique. This is straightforward and accurate enough when applied to the non-accreting eigenvalue equation (3.12) for moderate annular thicknesses, but for very large annuli and the accreting flows, $\delta\psi$ becomes a rapidly oscillating function in the outer regions due to its wave-like behaviour. It is therefore convenient to transform to a new independent variable defined by

$$Y = \frac{d\ln\delta\psi}{dr}. \tag{5.1}$$

The accreting and non-accreting perturbation equations (3.10) and (3.12) then become Riccati equations:

$$a^2(a^2-v_r^2)\left(\frac{dY}{dr}+Y^2\right)+\left(\frac{a^4}{r}+na^2\frac{da^2}{dr}-2i\bar{\sigma}a^2v_r+v_r^2\frac{da^2}{dr}-a^2v_r\frac{dv_r}{dr}\right)Y$$
$$+\left(\bar{\sigma}^2a^2-\frac{a^4m^2}{r^2}+i\bar{\sigma}v_r\frac{da^2}{dr}-a^2v_r im\frac{d\Omega}{dr}\right)=0 \tag{5.2}$$

$$a^2\left(\frac{dY}{dr}+Y^2\right)+\left(\frac{a^2}{r}+n\frac{da^2}{dr}\right)Y+\left(\bar{\sigma}^2-\frac{a^2m^2}{r^2}\right)=0 \tag{5.3}$$

where ϱ has been eliminated by using the polytropic relation

$$\varrho=\left(\frac{a^2}{\gamma K}\right)^n. \tag{5.4}$$

The polytropic index is chosen to be 3 in all the numerical work.

Equations (5.2) and (5.3) can be solved using the appropriate boundary conditions derived from those for $\delta\psi$. In the non-accreting case these are

$$Y=-\frac{\bar{\sigma}^2}{n}\left(\frac{da^2}{dr}\right)^{-1} \tag{5.5}$$

at each surface. In the accreting case at the sonic point,

$$Y=-\left(2ia^2\bar{\sigma}+a\frac{da^2}{dr}+2a^2\frac{dv_r}{dr}\right)^{-1}\left(\bar{\sigma}^2a-\frac{m^2a^3}{r^2}-\frac{2imla^2}{r^3}-i\bar{\sigma}\frac{da^2}{dr}\right), \tag{5.6}$$

while at infinity

$$Y=-i\sigma\left(\frac{n}{E}\right)^{1/2}. \tag{5.7}$$

To perform the integrations from infinity, the dependent variable is transformed to

$$y=\frac{r-r_s}{r+r_s-2} \tag{5.8}$$

so that as $r\to\infty$, $y\to1$ while $r=r_s$ corresponds to $y=0$.

Fig. 1 depicts the calculated eigenfrequencies for the $m=1$ modes, and is very similar to Glatzel's (1987) results for Newtonian annuli in pure rotation. As soon as the annulus is thickened away from the slender limit, the $N=0$ corotating mode goes unstable (the first hump in Fig. 1b). This is the surface wave interaction instability discussed by Blaes & Glatzel (1986) and Goldreich, Goodman & Narayan (1986). It stabilizes as the annulus gets thicker and merges with its complex conjugate damped partner (not shown in Fig. 1) to produce two stable modes. One of these then merges with the more rapidly rotating of the $N=1$ modes to form another unstable (the second hump in Fig. 1b) and damped (not shown) pair of modes. These again merge to produce two stable modes but the more rapidly rotating of the $N=2$ modes merges with one of these to create yet another complex conjugate pair. As the annulus gets thicker and thicker, higher and higher order modes join in this process until eventually the growth rate in Fig. 1(b) becomes a smooth function of E. The eigenfunction for one particular case in this regime is illustrated in Fig. 2, and it is clear that the effect of the higher order modes has been to make the eigenfunction wavelike in the outer regions of the annulus.

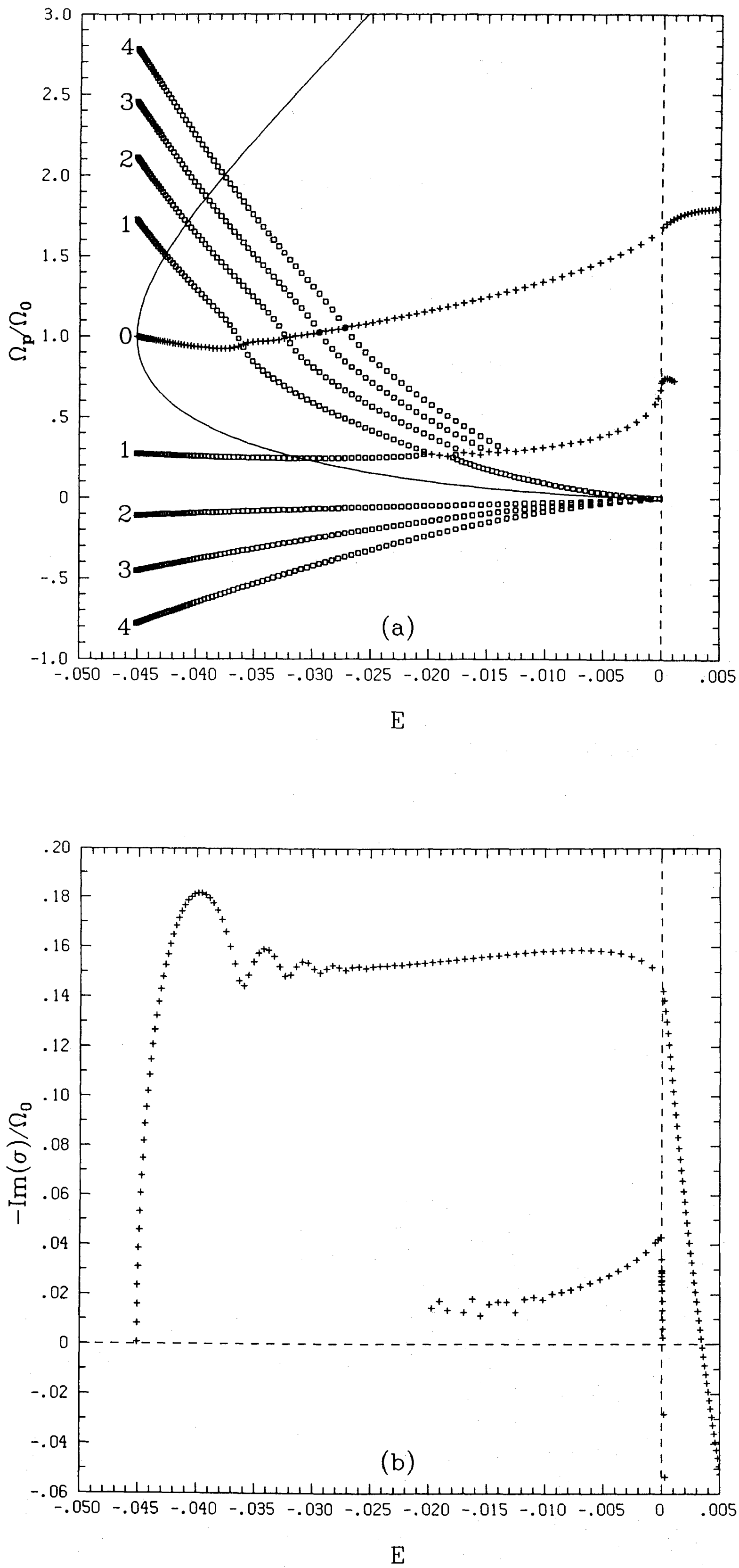

Figure 1. (a) Pattern speeds and (b) growth rates, scaled with respect to the angular velocity at r_{kep}, for the $m=1$ mode. The numbers to the left of each sequence of pattern speeds are the values of N, the number of nodes in the eigenfunction for that sequence in the slender annulus limit. The squares and crosses denote real and complex eigenfrequencies respectively. The solid curve gives the angular velocities at the edges of the annulus.

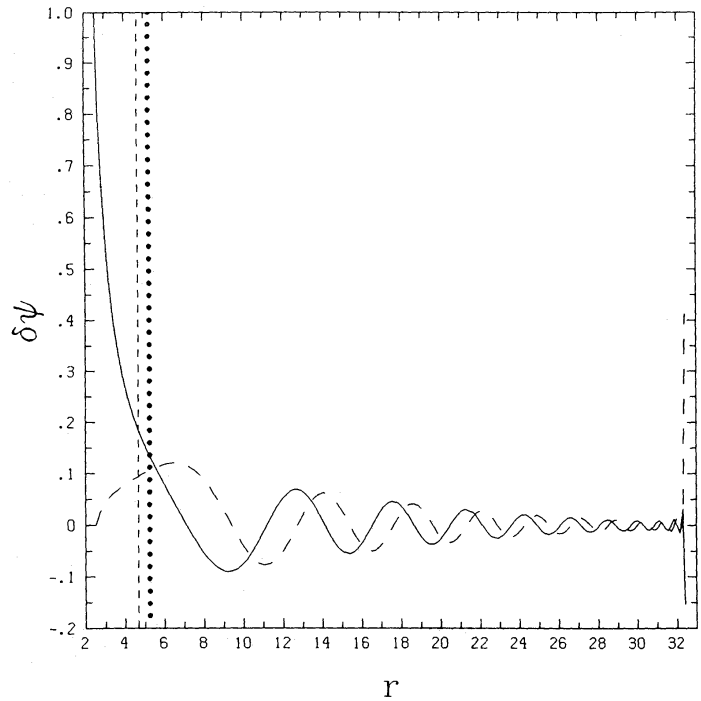

Figure 2. Real (continuous) and imaginary (dashed) parts of the eigenfunction for the fastest growing $m=1$ mode at $E=-0.014$. The figures have been normalized such that $\delta\psi$ is real and equal to unity at the inner edge. The dotted and short-dashed lines denote the positions of the pressure maximum (r_{kep}) and the corotation radius respectively.

For thick annuli the instability is best interpreted in terms of a trapped mode between the inner radius and corotation which radiates a wave into the outer region. Such modes have been discussed at length by Narayan, Goldreich & Goodman (1987). the region inside corotation acts as a reservoir of negative angular momentum and the outward propagating wave leaks positive angular momentum out of this region, thereby fuelling the perturbation growth.

In addition to the sequence of unstable modes which starts with the $N=0$ corotating mode, there is another sequence which starts at a finite, non-zero annular thickness and is produced by a merging of the slowly rotating $N=1$ mode with the stable mode produced by the coalescence of the $N=0$ damped and unstable modes. The behaviour of this instability is similar. As E increases it stabilizes but then a merging with another stable mode produces another unstable and damped pair, and this continues out to infinitely thick annuli. The eigenfunction for such a mode is illustrated in Fig. 3. In the outer regions we again have an outward propagating wave but the inner regions are slightly more complicated. A node has been added as a result of the slowly rotating $N=1$ mode which helped produce this sequence.

As the annulus starts to accrete both unstable modes quickly stabilize and then become damped. Very little accretion is required – the more rapidly growing mode is stabilized when $E=0.00346$, corresponding to a sonic radius $r_s=1.998$. The ratios of radial to azimuthal velocities at the sonic radius and at r_{kep} are 0.03 and $\sim 10^{-5}$ respectively. Clearly, the flow is still in a state of almost pure rotation outside the sonic point.

No further unstable $m=1$ modes appear to exist for non-accreting annuli as all the stable modes which could merge to produce unstable modes only to do so as the annulus becomes very large. If they do merge, then the resulting unstable modes have zero pattern speeds, and therefore have corotation points at very large radii. It is impossible to treat such modes numerically, and no attempt has been made to follow them into the accretion regime. Indeed, it

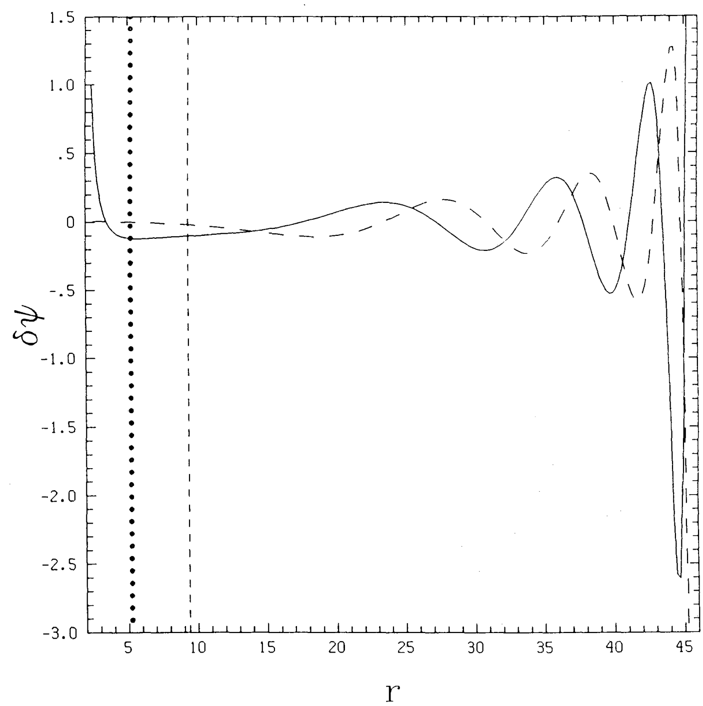

Figure 3. Real and imaginary parts of the eigenfunction of the more slowly growing $m=1$ mode at $E=-0.010$. The normalization is again chosen such that $\delta\psi=1$ at the inner edge.

may be that the normal mode assumption breaks down for at least some of these modes at the transition point $E=0$.

The $m=-1$ modes have also been examined and a very similar behaviour occurs. Attempts have been made to follow higher $|m|$ modes through the accretion transition but it has proved difficult to find any which are unstable. This could be explained if the modes are damped very quickly when the accretion starts but problems with numerical convergence onto unstable eigenvalues cannot be ruled out.

6 Angular momentum transport

The mechanism which drives instabilities in the differentially rotating annuli is the outward transport of angular momentum by non-axisymmetric modes across their corotation points. This allows the modes to reduce the shear energy of the equilibrium flow and thereby fuel their own growth.

At first sight the rapidity with which accretion damps out the unstable modes is rather surprising. Negative angular momentum must be advected out of the inner region faster than positive angular momentum is being leaked through corotation in order for this damping to occur. That this is actually occurring can be seen from a direct calculation of the angular momentum transport, which also provides a check on the numerical results of the previous section.

The full time-dependent perturbation equation (3.9) may be derived by extremizing the functional

$$H=\int rL\,dr\,dt\,d\phi \tag{6.1}$$

where the Lagrangian density is (Moncrief 1980)

$$L=\frac{1}{2}\left[\varrho\delta\psi_{,r}^2+\frac{\varrho}{r^2}\delta\psi_{,\phi}^2-\frac{\varrho}{a^2}(\delta\psi_{,t}+v_r\delta\psi_{,r}+\Omega\delta\psi_{,\phi})^2\right]. \tag{6.2}$$

Here the commas denote partial derivatives. Because L has no explicit t- or ϕ-dependence, Noether's theorem implies the existence of two conserved quantities corresponding to the energy and angular momentum carried by the perturbations. The angular momentum equation takes the form

$$\frac{\partial J}{\partial t}+\frac{1}{r}\frac{\partial}{\partial r}(rF_r)+\frac{1}{r}\frac{\partial F_\phi}{\partial \phi}=0 \tag{6.3}$$

where the angular momentum density and flux components are given by

$$J=\frac{\partial L}{\partial \delta\psi_{,t}}\delta\psi_{,\phi}=-\frac{\varrho}{a^2}\delta\psi_{,\phi}(\delta\psi_{,t}+v_{\mathrm{r}}\delta\psi_{,r}+\Omega\delta\psi_{,\phi}), \tag{6.4}$$

$$F_r=\frac{\partial L}{\partial \delta\psi_{,r}}\delta\psi_{,\phi}=\delta\psi_{,\phi}\left[\varrho\delta\psi_{,r}-\frac{\varrho}{a^2}v_{\mathrm{r}}(\delta\psi_{,t}+v_{\mathrm{r}}\delta\psi_{,r}+\Omega\delta\psi_{,\phi})\right], \tag{6.5}$$

$$F_\phi=\left(\frac{\partial L}{\partial \delta\psi_{,\phi}}\delta\psi_{,\phi}-L\right)r. \tag{6.6}$$

Note that equations (3.8) and (6.4) together imply $J=r\delta\varrho\delta v_\phi$. Integrating equation (6.3) over azimuth,

$$\frac{\partial \bar{J}}{\partial t}+\frac{1}{r}\frac{\partial}{\partial r}(r\bar{F}_r)=0 \tag{6.7}$$

where $\bar{J}$ and $\bar{F}_r$ are azimuthally averaged quantities:

$$\bar{J}\equiv\frac{1}{2\pi}\int_0^{2\pi}J\,d\phi \tag{6.8}$$

$$\bar{F}_r\equiv\frac{1}{2\pi}\int_0^{2\pi}F_r\,d\phi. \tag{6.9}$$

For normal mode solutions these become

$$\bar{J}=-\frac{\varrho m}{2a^2}\left[m(\Omega-\Omega_{\mathrm{p}})\,|\delta\psi|^2+i\frac{v_{\mathrm{r}}}{2}\left(\delta\psi\frac{\partial\delta\psi^*}{\partial r}-\delta\psi^*\frac{\partial\delta\psi}{\partial r}\right)\right] \tag{6.10}$$

and

$$\bar{F}_{\mathrm{r}}=\frac{\varrho m}{2a^2}\left[-v_{\mathrm{r}}m(\Omega-\Omega_{\mathrm{p}})|\delta\psi|^2+\frac{i}{2}(a^2-v_{\mathrm{r}}^2)\left(\delta\psi\frac{\partial\delta\psi^*}{\partial r}-\delta\psi^*\frac{\partial\delta\psi}{\partial r}\right)\right] \tag{6.11}$$

while the transport equation may be written

$$-2\,\mathrm{Im}(\sigma)\bar{J}+\frac{1}{r}\frac{\partial}{\partial r}(r\bar{F}_r)=0. \tag{6.12}$$

In deriving equations (6.10) and (6.11) it must be remembered that the real part of $\delta\psi$ must be taken before evaluating J and F_r. Note that in the case of the non-accreting annulus (and even in the accreting flows considered here because v_{r} is so small), $\bar{J}$ vanishes at corotation, being negative inside and positive outside. Physically, this simply means that the mode carries negative angular momentum with respect to the more rapidly rotating equilibrium flow inside corotation while the opposite is true outside. Note also that $r\bar{F}_r$ has a turning point wherever $\bar{J}=0$.

Integrating equation (6.12) between two radii r_a and r_b and solving for the growth rate,

$$-\operatorname{Im}(\sigma)=\frac{[r\bar{F}_r]_{r_b}^{r_a}}{2\int_{r_a}^{r_b} r\bar{J}\,dr}. \tag{6.13}$$

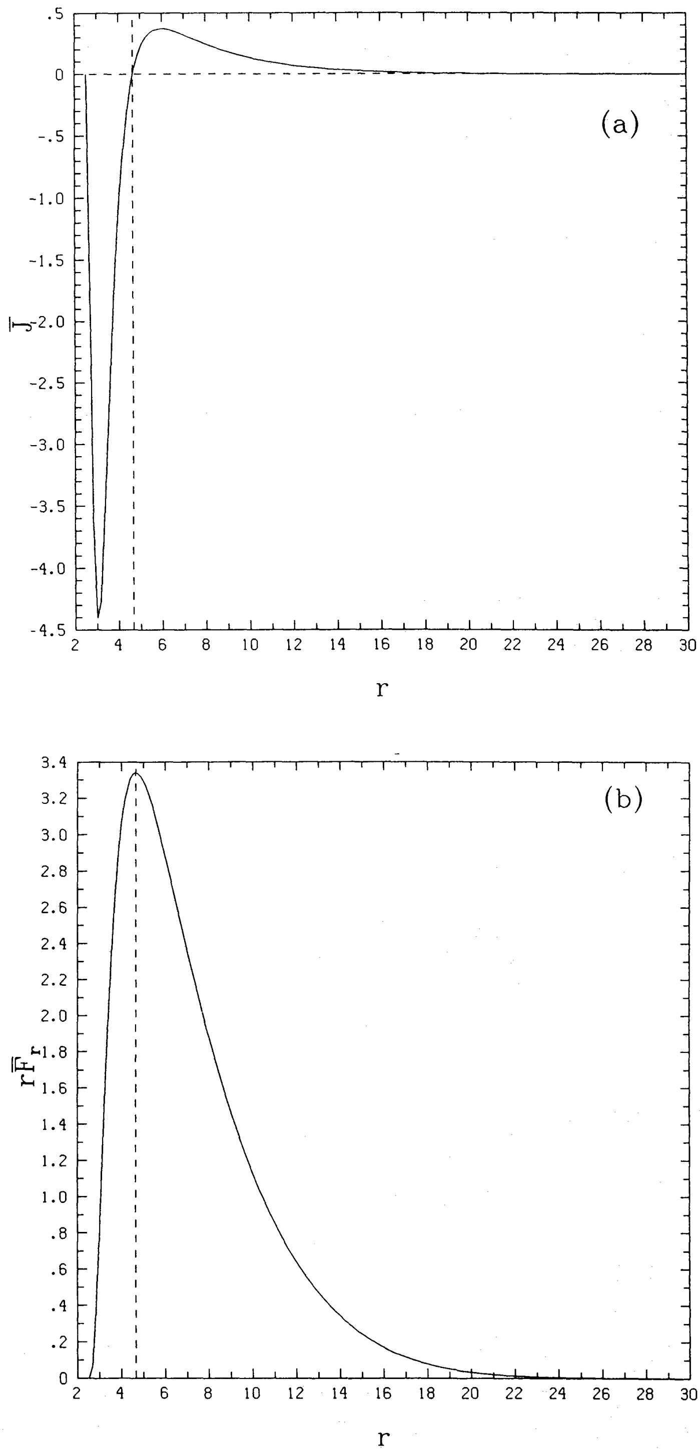

Figure 4. Azimuthally averaged (a) angular momentum density $\bar{J}$ and (b) angular momentum crossing a given radius per unit time $r\bar{F}_r$ for the fastest growing $m=1$ mode at $E=-0.014$. The dashed line indicates the position of the corotation radius. (N.B. The vertical scales here are arbitrary and have been chosen for clarity.)

In the case of a non-accreting annulus equation (6.11) implies that $\bar{F}_r$ vanishes at the surface radii. Taking r_a to be either of these and r_b to be the corotation radius, then equation (6.13) gives the expected result that a positive outward flux of angular momentum at corotation is required for instability. If this is the case then even if the annulus extends to infinity and angular momentum is radiated away, the flow would still be unstable because the region inside corotation would be losing angular momentum to the outside (Papaloizou & Pringle 1987). Accretion can stabilize the

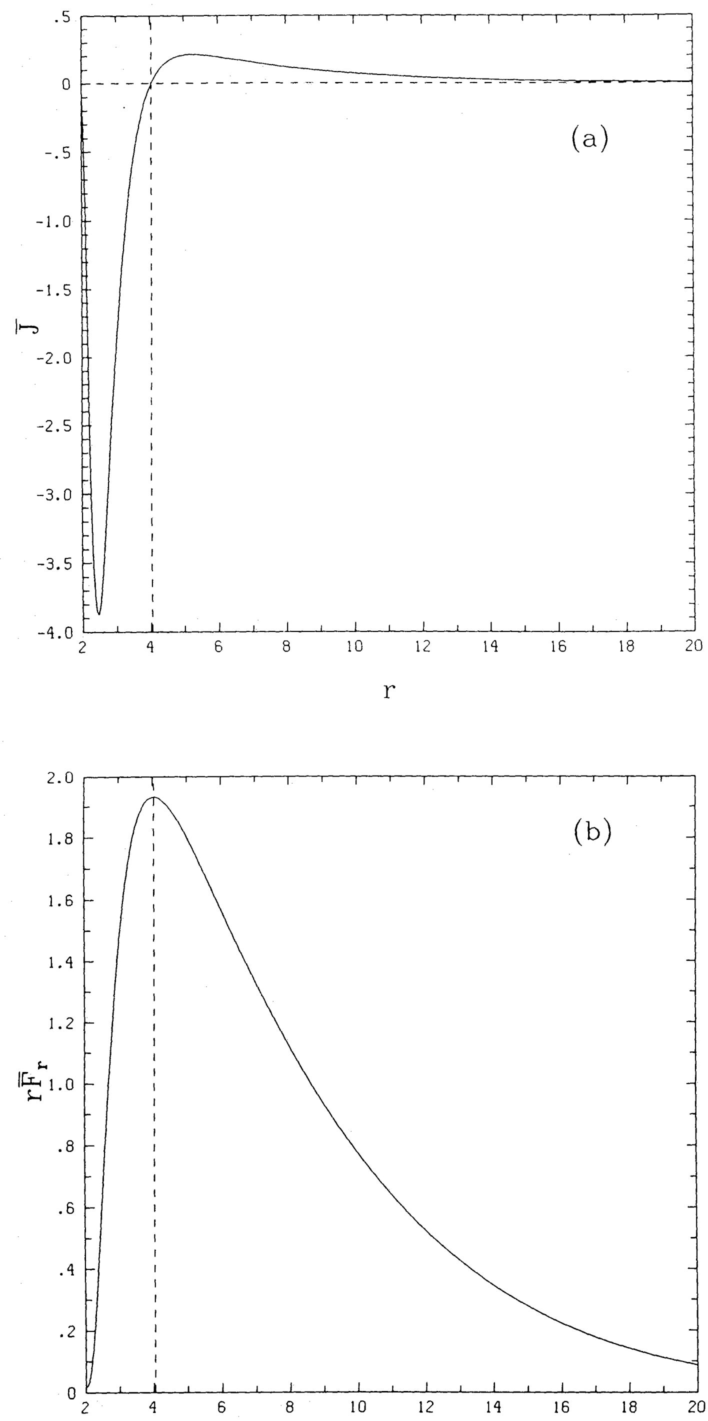

Figure 5. The same as Fig. 4 but for the barely accreting flow $E=-0.0001$.

flow by advecting negative angular momentum inward through the sonic point faster that positive angular momentum is being leaked out through corotation.

Figs 4 and 5 depict $\bar{J}$ and $r\bar{F}_r$ for the fastest growing unstable modes of a thick annulus and a barely accreting flow. The large positive value of $r\bar{F}_r$ at corotation drives the instability, but as E is increased there is more accretion and the mode is eventually damped (Fig. 6).

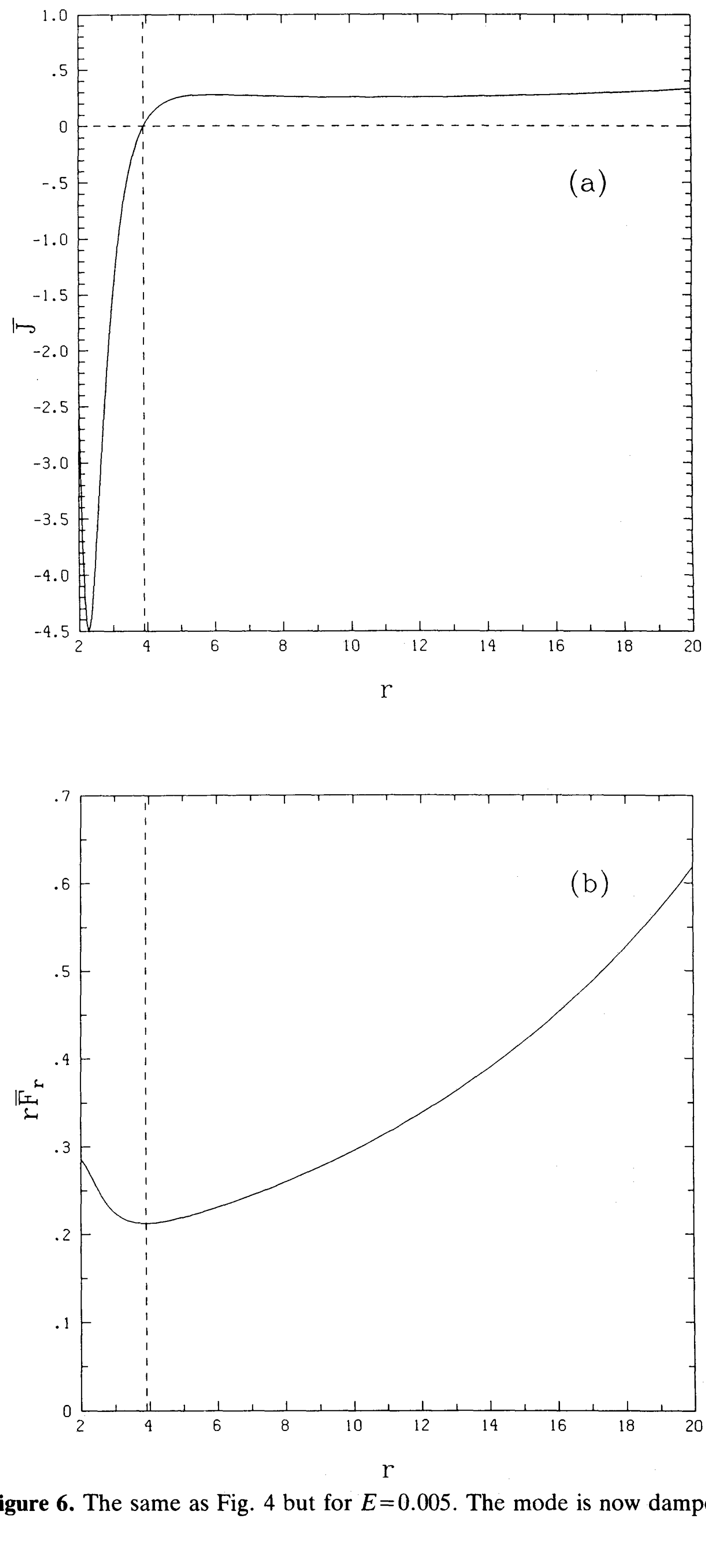

Figure 6. The same as Fig. 4 but for $E=0.005$. The mode is now damped.

7 Discussion

The primary conclusion of this paper is that accretion can exert a strong damping influence which has not yet been considered in any of the previous studies of dynamical instabilities in thick discs. Of course the flow considered in this paper is only a toy model which is easy to analyse, but this is offset somewhat by the fact that in certain ways it is the model most prone to be unstable. Specific angular momentum gradients (which can exist in a barotropic accreting flow only if there is non-zero viscosity) tend to reduce the growth rate of constant specific angular momentum modes (Papaloizou & Pringle 1985; Glatzel 1987). The fastest growing unstable modes of thick *tori* have smaller growth rates than those of thick annuli (Kojima 1986a; Frank, private communication). Finally, the gravitational redshift of a real black hole acts to reduce growth rates (Kojima 1986b).

However, in two dimensions accretion almost certainly has an enhanced dynamical importance compared to what it would have in a thick disc flow. In particular, the transonic steam leaves the disc only in the equatorial plane, and so the funnels might still provide an effective inner edge for unstable modes. Even so, accretion will still have a damping effect and this will be strongest for those modes which are concentrated towards the inner equatorial edge, which is precisely what is observed for the fastest growing modes (Kojima 1986a; Frank, private communication). It may be that these could be stabilized and that only modes with more vertical structure, or which are concentrated in the outer regions, would survive. These will have slower growth rates and it is conceivable that they would generate turbulence at a level sufficient to drive the stabilizing accretion flow. Clearly more work should be directed along these lines.

Acknowledgments

It is a pleasure to acknowledge many useful discussions with Juhan Frank, Peter Goldreich, John Hawley and Sterl Phinney. The original emphasis of accretion as being of some importance is due to Marek Abramowicz, who suggested this project to me. Finally, many thanks are due to Wolfgang Glatzel for his help and advice on numerical problems and for communicating his results to me long before publication. Financial support was provided by a SERC overseas studentship, a Chaim Weizmann postdoctoral fellowship from Caltech and NSF grant AST84-15355. This work was begun at the International School Studies, Trieste.

References

Abramowicz, M. A., Blaes, O. M. & Lu, J., 1986. In: *Structure and Evolution of Active Galactic Nuclei,* p. 113, ed. Giuricin, G., Reidel, Dordrecht, Holland.
Abramowicz, M. A. & Zurek, W. H., 1982. *Astrophys. J.,* **246,** 314.
Balbinski, E., 1982. *PhD thesis,* University of Wales.
Blaes, O. M., 1985. *Mon. Not. R. astr. Soc.,* **216,** 553.
Blaes, O. M. & Glatzel, W., 1986. *Mon. Not. R. astr. Soc.,* **220,** 253.
Broadbent, E. G. & Moore, D. W., 1979. *Phil. Trans. R. Soc. Lond. A,* **290,** 353.
Drury, L. O'C., 1985. *Mon. Not. R. astr. Soc.,* **217,** 821.
Dyson, J. & Schutz, B. F., 1979. *Proc. R. Soc. Lond. A,* **368,** 389.
Glatzel, W., 1987. *Mon. Not. R. astr. Soc.,* **225,** 227.
Goldreich, P., Goodman, J. & Narayan, R., 1986. *Mon. Not. R. astr. Soc.,* **221,** 339.
Goldreich, P. & Narayan, R., 1985. *Mon. Not. R. astr. Soc.,* **213,** 7P.
Goodman, J., Narayan, R. & Goldreich, P., 1987. *Mon. Not. R. astr. Soc.,* **225,** 695.
Hawley, J. F., 1987. *Mon. Not. R. astr. Soc.,* **225,** 677.
Kato, S., 1987. Preprint.
Kojima, Y., 1986a. *Prog. theor. Phys., Osaka,* **75,** 251.
Kojima, Y., 1986b. *Prog. theor. Phys., Osaka,* **75,** 1464.
Loska, Z., 1986. *Acta astr.,* **36,** 43.
Moncrief, V., 1980. *Astrophys. J.,* **235,** 1038.
Narayan, R., Goldreich, P. & Goodman, J., 1987. Preprint.
Paczynski, B. & Wiita, P. J., 1980. *Astr. Astrophys.,* **88,** 23.

Papaloizou, J. C. B. & Pringle, J. E., 1984. *Mon. Not. R. astr. Soc.*, **208**, 721.
Papaloizou, J. C. B. & Pringle, J. E., 1985. *Mon. Not. R. astr. Soc.*, **213**, 799.
Papaloizou, J. C. B. & Pringle, J. E., 1987. *Mon. Not. R. astr. Soc.*, in press.
Rees, M. J., 1984. *Ann. Rev. Astr. Astrophys.*, **22**, 471.
Tassoul, J.-L., 1978. *Theory of Rotating Stars*, Princeton University Press.
Zurek, W. H. & Benz, W., 1986. *Astrophys. J.*, **308**, 123.

Appendix: Axisymmetric stability of two-dimensional accreting flows

It is easy to generalize Moncrief's (1980) proof of the stability of spherical accretion to axisymmetric perturbations of the flows considered in this paper. 'Axisymmetric' of course refers to Eulerian variables, so that actually the perturbed velocity potential could in principle be a linear function of ϕ:

$$\delta\psi=\delta\psi'(t,r)+C\phi \tag{A1}$$

where C is a constant. Non-zero C implies a perturbation in the specific angular momentum which is everywhere constant, and is therefore equivalent to perturbing a stationary flow with slightly different specific angular momentum. We therefore assume that $C=0$.

Noether's theorem then gives the following formulae for the energy density and radial energy flux

$$\mathscr{E}=\frac{\varrho}{2}\left[\frac{1}{a^2}\delta\psi_{,t}^2+\left(1-\frac{v_{\mathrm{r}}^2}{a^2}\right)\delta\psi_{,r}^2\right], \tag{A2}$$

$$F_r^E=\varrho v_{\mathrm{r}}\left[\frac{1}{a^2}\delta\psi_{,t}^2-\left(1-\frac{v_{\mathrm{r}}^2}{a^2}\right)\delta\psi_{,t}\delta\psi_{,r}\right]. \tag{A3}$$

The total perturbed energy of the flow outside the sonic point is therefore

$$\mathscr{E}_{\mathrm{tot}}=\frac{1}{2}\int_0^{2\pi}\int_{r_{\mathrm{s}}}^{\infty} r\frac{\varrho}{a^2}[\delta\psi_{,t}^2+(a^2-v_{\mathrm{r}}^2)\delta\psi_{,r}^2]\,dr\,d\phi \tag{A4}$$

which is a positive definite quantity. Here we restrict consideration to perturbations which decay fast enough so that $\mathscr{E}_{\mathrm{tot}}$ is finite:

$$\delta\psi_{,t}\sim r^{-(1+\delta)} \qquad \delta\psi_{,r}\sim r^{-(1+\delta)} \tag{A5}$$

where $\delta>0$.

The energy transport equation,

$$\frac{\partial\mathscr{E}}{\partial t}+\frac{1}{r}\frac{\partial}{\partial r}(rF_r^E)+\frac{1}{r}\frac{\partial}{\partial\phi}(F_\phi^E)=0, \tag{A6}$$

can be integrated to give the time rate of change of $\mathscr{E}_{\mathrm{tot}}$:

$$\frac{d\mathscr{E}_{\mathrm{tot}}}{dt}=\int_0^{2\pi}d\phi\left\{r\varrho v_{\mathrm{r}}\left[\frac{1}{a^2}\delta\psi_{,t}^2-\left(1-\frac{v_{\mathrm{r}}^2}{a^2}\right)\delta\psi_{,t}\delta\psi_{,r}\right]\right\}_{r_{\mathrm{s}}}^{\infty}. \tag{A7}$$

The right-hand side vanishes as $r\to\infty$ and so

$$\frac{d\mathscr{E}_{\mathrm{tot}}}{dt}=-\int_0^{2\pi}d\phi\frac{r_{\mathrm{s}}}{a_{\mathrm{s}}}(\varrho\delta\psi_{,t}^2)|_{r_{\mathrm{s}}}<0. \tag{A8}$$

Hence $\mathscr{E}_{\mathrm{tot}}$, viewed as a positive definite norm of the perturbations, always decays and so the flow is stable to axisymmetric perturbations. It should be pointed out that this sort of proof fails if both the stationary and perturbed velocity fields have non-zero components tangential to the sound horizon. Indeed, the barely accreting flow which is unstable to non-axisymmetric perturbations is a good example of this.